MIT Libraries | DSpace@MIT

MIT Open Access Articles

Calculating the band structure of 3C-SiC using sp[superscript 3]d[superscript 5]s* + Δ model

Massachusetts Institute of Technology

RESEARCH

Calculating the band structure of 3C-SiC using $sp^3d^5s^*+\Delta$ model

Murat Onen[1] · Marco Turchetti[1]

Abstract

We report on a semiempirical tight-binding model for 3C-SiC including the effect of $sp^3d^5s^*$ orbitals and spin–orbit coupling (Δ). In this work, we illustrate in detail the method to develop such a model for semiconductors with zincblende structure, based on Slater–Koster integrals, and we explain the optimization method used to fit the experimental results with such a model. This method shows high accuracy for the evaluation of 3C-SiC band diagram in terms of both the experimental energy levels at high symmetry points and the effective masses.

Introduction

Silicon carbide (SiC) exhibits strong chemical bonding and physical stability. The 3C polytype of SiC is of particular interest due to its superior electronic properties such as high electron mobility and saturation velocity which make it a perfect candidate for building devices that have to withstand harsh environments [1–3]. In particular, it is widely used in high-voltage and high-temperature semiconductor industries, in astronomy, and, as it is resistant to radiation, in nuclear reactors [4]. Therefore, the understanding of its electronic structure is critical for the improvement in existing SiC-based technologies and the development of new applications.

Several models have been previously used to fit the experimental data to reconstruct SiC band diagram, including density functional theory (DFT) with local density approximation (LDA) [5, 6], Hartree–Fock–Slater model using discrete variational method [7], and empirical pseudopotential method [8, 9]. This work implements a semiempirical tight-binding model (SETBM) for fitting experimental data

to calculate the band structure of semiconductors, which proved its reliability through the years.

The SETBM approach has previously been applied for SiC in the literature but was limited to only including sp^3 orbitals, entailing an 8×8 Hamiltonian matrix [6]. To improve the capacity of the model, an excited orbital s^* has been included as well [10]. However, the inclusion of the d orbitals and the spin–orbit coupling (Δ) is required to portray the electron band structure in a more complete way that accounts for the splitting of the bands due to the lifted degeneracy with the spin–orbit coupling (SOC) effects. In this work, we propose an $sp^3d^5s^*+\Delta$ model for 3C-SiC based on Slater–Koster integrals [11]. Similar models have been applied for III–V semiconductors by Jancu et al. [12]. We first show how to construct the resulting 40×40 Hamiltonian matrix and then how to optimize it using the experimental data. We validate the model's accuracy by first implementing it for GaAs and comparing it with the results found in Ref. [12]. Modeling and optimization steps are clearly shown, such that it can be implemented for other materials as well.

Semiempirical tight-binding method (SETBM) for zincblende structures

To evaluate the band diagram of 3C-SiC, we build the Hamiltonian matrix using the linear combination of atomic orbitals (LCAO) model, considering only the nearest neighbor interactions which collapse the overlap matrix to identity.

Murat Onen and Marco Turchetti contributed equally to this work.

✉ Murat Onen
   monen@mit.edu

✉ Marco Turchetti
   turchett@mit.edu

[1] Research Laboratory of Electronics, Massachusetts Institute of Technology, Cambridge, MA 02139, USA

*sp³d⁵s** **Model**

The tight-binding Hamiltonian matrix is built by evaluating each interaction integral $H_{jk} = \left\langle \Phi_j | \hat{H} | \Phi_k \right\rangle$ between the nearest neighbor orbitals. In this notation, $|\Phi_i\rangle$ are the $s, p, d,$ and s^* orbitals and $\hat{H}$ is the full crystal interaction Hamiltonian. Using ten orbitals $(s, p_x, p_y, p_z, d_x, d_y, d_z, d_{x^2-y^2}, d_{3r^2-z^2})$ for two atoms (cation: Si^+ and anion: C^-) results in a Hamiltonian matrix of 20×20 before the inclusion of SOC.

To evaluate these integrals, we adopted the Slater–Koster notation [11] using $l = m = n = -\frac{1}{\sqrt{3}}$ as 3C-SiC has a zinc-blende crystal structure. Figure 1 shows the resulting 20×20 Hamiltonian matrix. Matrix entries are calculated as follows:

$$V_{ss} = V_{ss\sigma}$$

$$V_{sp} = -\frac{1}{\sqrt{3}} V_{sp\sigma}$$

$$V_{xx} = \frac{1}{3} V_{pp\sigma} + \frac{2}{3} V_{pp\pi}$$

$$V_{xy} = \frac{1}{3} V_{pp\sigma} - \frac{1}{3} V_{pp\pi}$$

$$V_{sd} = \frac{1}{\sqrt{3}} V_{sd\sigma}$$

$$V_{pd} = \frac{1}{3} \left[V_{pd\sigma} - \frac{2}{\sqrt{3}} V_{pd\pi} \right]$$

$$U_{pd} = \frac{1}{3} \left[V_{pd\sigma} + \frac{1}{\sqrt{3}} V_{pd\pi} \right]$$

$$W_{pd} = \frac{2}{3} V_{pd\pi}$$

$$V_{dd} = \frac{1}{9} \left[3V_{dd\sigma} + 2V_{dd\pi} + 4V_{dd\delta} \right]$$

$$\widetilde{V}_{dd} = \frac{1}{3} \left[2V_{dd\pi} + V_{dd\delta} \right]$$

$$U_{dd} = \frac{1}{9} \left[3V_{dd\sigma} - V_{dd\pi} - 2V_{dd\delta} \right]$$

$$W_{dd} = \frac{2}{3\sqrt{3}} \left[-V_{dd\pi} + V_{dd\delta} \right].$$

The α and β superscripts used in Fig. 1 define whether it refers to an anion-to-cation integral or a cation-to-anion one. Diagonal elements (E_{ii}) denote the self-integrals of the orbitals. The s^* integrals use the same notation of the s ones. The g_i are the phase factors that take into account the fact that we are evaluating integrals with respect to each nearest neighbor, which are defined as:

$$g_0 = 1 + e^{-ikR_1} + e^{-ikR_2} + e^{-ikR_3}$$

$$g_1 = 1 + e^{-ikR_1} - e^{-ikR_2} - e^{-ikR_3}$$

$$g_2 = 1 - e^{-ikR_1} + e^{-ikR_2} - e^{-ikR_3}$$

$$g_3 = 1 - e^{-ikR_1} - e^{-ikR_2} + e^{-ikR_3}$$

w h e r e $R_1 = \left[-\frac{a}{2}, -\frac{a}{2}, 0 \right]$, $R_2 = \left[0, -\frac{a}{2}, -\frac{a}{2} \right]$, $R_1 = \left[-\frac{a}{2}, 0, -\frac{a}{2} \right]$, and a is the lattice constant.

Spin–orbit coupling

In this model, we also take into account the spin–orbital coupling between p orbitals as explained by Datta [13]. Spin-orbit interaction is responsible for lifting the degeneracy of the valence band and plays a role in defining the optical properties of the material [6]. In this work, we considered only the contribution of p valence states since that of the excited d states is much smaller [12].

The introduction of spin–orbit interaction in the model is implemented distinguishing between ↑ and ↓ electrons and creating a matrix twice the rank with the introduction of two coupling parameters δ_a and δ_c (where $\delta_{a,c} = \Delta_{a,c}/3$). Such a 40×40 Hamiltonian matrix, H, can be defined starting from a matrix having two of the 20×20 $H_{sp^3d^5s^*}$ matrices portrayed in Fig. 1 as diagonal elements and adding it to a coupling matrix H^Δ:

$$H = \begin{bmatrix} H_{sp^3d^5s^*} & 0 \\ 0 & H_{sp^3d^5s^*} \end{bmatrix} + \begin{bmatrix} H_{11}^\Delta & H_{12}^\Delta \\ H_{21}^\Delta & H_{22}^\Delta \end{bmatrix}$$

where H_{ij}^Δ are defined in Fig. 2.

Verification of the model

The model involving $sp^3d^5s^* + \Delta$ parameters has previously been applied to a set of semiconductors in Ref. [12]. As a verification of the model construction and optimization procedure of the coupling parameters, here we demonstrate the results obtained for GaAs. Table 1 shows that the coupling parameters and the accuracy of our model are comparable to those reported in Ref. [12].

Fig. 1 $20 \times 20\, H_{sp^3d^5s^*}$ matrix

$H^\Delta_{11} =$

	ϕ^a_s	ϕ^c_s	$\phi^a_{p(x)}$	$\phi^a_{p(y)}$	$\phi^a_{p(z)}$	$\phi^c_{p(x)}$	$\phi^c_{p(y)}$	$\phi^c_{p(z)}$	$\cdots$
$\phi^c_{p(z)}$	0	0	0	0	0	0	0	0	
$\phi^c_{p(y)}$	0	0	0	0	0	$-i\delta_c$	0	0	
$\phi^c_{p(x)}$	0	0	0	0	0	0	$i\delta_c$	0	
$\phi^a_{p(z)}$	0	0	0	0	0	0	0	0	
$\phi^a_{p(y)}$	0	0	$-i\delta_a$	0	0	0	0	0	$\cdots$
$\phi^a_{p(x)}$	0	0	0	$i\delta_a$	0	0	0	0	
ϕ^c_s	0	0	0	0	0	0	0	0	
ϕ^a_s	0	0	0	0	0	0	0	0	
$\vdots$				$\vdots$					$\ddots$

$H^\Delta_{12} =$

	ϕ^a_s	ϕ^c_s	$\phi^a_{p(x)}$	$\phi^a_{p(y)}$	$\phi^a_{p(z)}$	$\phi^c_{p(x)}$	$\phi^c_{p(y)}$	$\phi^c_{p(z)}$	$\cdots$
$\phi^c_{p(z)}$	0	0	0	0	0	δ_c	$-i\delta_c$	0	
$\phi^c_{p(y)}$	0	0	0	0	0	0	0	$i\delta_c$	
$\phi^c_{p(x)}$	0	0	0	0	0	0	0	$-\delta_c$	
$\phi^a_{p(z)}$	0	0	δ_a	$-i\delta_a$	0	0	0	0	
$\phi^a_{p(y)}$	0	0	0	0	$i\delta_a$	0	0	0	$\cdots$
$\phi^a_{p(x)}$	0	0	0	$-\delta_a$	0	0	0	0	
ϕ^c_s	0	0	0	0	0	0	0	0	
ϕ^a_s	0	0	0	0	0	0	0	0	
$\vdots$				$\vdots$					$\ddots$

$H^\Delta_{21} =$

	$\overline{\phi}^a_s$	$\overline{\phi}^c_s$	$\overline{\phi}^a_{p(x)}$	$\overline{\phi}^a_{p(y)}$	$\overline{\phi}^a_{p(z)}$	$\overline{\phi}^c_{p(x)}$	$\overline{\phi}^c_{p(y)}$	$\overline{\phi}^c_{p(z)}$	$\cdots$
$\phi^c_{p(z)}$	0	0	0	0	0	$-\delta_c$	$-i\delta_c$	0	
$\phi^c_{p(y)}$	0	0	0	0	0	0	0	$i\delta_c$	
$\phi^c_{p(x)}$	0	0	0	0	0	0	0	δ_c	
$\phi^a_{p(z)}$	0	0	$-\delta_a$	$-i\delta_a$	0	0	0	0	
$\phi^a_{p(y)}$	0	0	0	0	$i\delta_a$	0	0	0	$\cdots$
$\phi^a_{p(x)}$	0	0	0	δ_a	0	0	0	0	
ϕ^c_s	0	0	0	0	0	0	0	0	
ϕ^a_s	0	0	0	0	0	0	0	0	
$\vdots$				$\vdots$					$\ddots$

$H^\Delta_{22} =$

	$\overline{\phi}^a_s$	$\overline{\phi}^c_s$	$\overline{\phi}^a_{p(x)}$	$\overline{\phi}^a_{p(y)}$	$\overline{\phi}^a_{p(z)}$	$\overline{\phi}^c_{p(x)}$	$\overline{\phi}^c_{p(y)}$	$\overline{\phi}^c_{p(z)}$	$\cdots$
$\overline{\phi}^c_{p(z)}$	0	0	0	0	0	0	0	0	
$\overline{\phi}^c_{p(y)}$	0	0	0	0	0	$i\delta_c$	0	0	
$\overline{\phi}^c_{p(x)}$	0	0	0	0	0	0	$-i\delta_c$	0	
$\overline{\phi}^a_{p(z)}$	0	0	0	0	0	0	0	0	
$\overline{\phi}^a_{p(y)}$	0	0	$i\delta_a$	0	0	0	0	0	$\cdots$
$\overline{\phi}^a_{p(x)}$	0	0	0	$-i\delta_a$	0	0	0	0	
$\overline{\phi}^c_s$	0	0	0	0	0	0	0	0	
$\overline{\phi}^a_s$	0	0	0	0	0	0	0	0	
$\vdots$				$\vdots$					$\ddots$

Fig. 2 Spin–orbit matrix

Table 1 Comparison between experimental values of the GaAs high symmetry points and effective masses, the corresponding values evaluated by Jancu et al. in Ref. [12] using SETBM and the same value evaluated using our model

Parameter	Previous work [12]	This work	Experimental [6]
Γ_{6v}	−12.910 eV	−13.070 eV	−13.1 eV
$-\Delta_0$	−0.340 eV	−0.339	−0.341 eV
Γ_{6c}	1.519 eV	1.519 eV	1.519 eV
Γ_{7c}	4.500 eV	4.497 eV	4.53 eV
Γ_{8c}	4.716 eV	4.764 eV	4.716 eV
X_{6v}	−3.109 eV	−2.904 eV	−2.88 eV
X_{7c}	−2.929 eV	−2.790 eV	−2.80 eV
X_{6c}	1.989 eV	2.009 eV	1.98 eV
X_{7c}	2.328 eV	2.385 eV	2.35 eV
L_{6v}	−1.330 eV	−1.427 eV	−1.42 eV
$L_{4,5v}$	−1.084 eV	−1.180 eV	−1.20 eV
L_{6c}	1.837 eV	1.829 eV	1.85 eV
L_{7c}	5.047 eV	5.303 eV	5.47 eV
$m(\Gamma_{6c})$	0.067 m_0	0.067 m_0	0.067 m_0
Avg. accuracy	97.11%	99.45%	100%

Table 2 Comparison between experimental values of the SiC high symmetry points and effective masses, the corresponding values evaluated by Theodorou et al. in Ref. 6 using SETBM and the same value evaluated using our model

Parameter	Previous work [6]	This work	Experimental [6]
Δ_0	–	− 10.3600 meV	− 10.36 meV
Γ_{1c}	7.07 eV	7.4000 eV	7.40 eV
Γ_{15c}	8.98 eV	7.7253 eV	7.75 eV
X_{5v}	− 3.2 eV	− 3.5977 eV	− 3.60 eV
X_{1c}	2.47 eV	2.3900 eV	2.39 eV
X_{3c}	5.64 eV	5.5000 eV	5.50 eV
L_{3v}	− 1.18 eV	− 1.1522 eV	− 1.16 eV
L_{1c}	6.22 eV	5.9400 eV	5.94 eV
L_{3c}	9.11 eV	8.5004 eV	8.50 eV
$m\parallel$	–	$0.6700m_0$	$0.67m_0$
$m_\perp$	–	$0.2500m_0$	$0.25m_0$
Avg. Accuracy	93.6%	99.91%	100%

Optimization for SiC

Following the construction of the matrix, an optimization procedure is necessary to find the SETBM parameters for any given material. Here we provide a method that can be generalized to other materials as well. The optimization requires experimental data on energy levels at high symmetry points and effective masses in certain directions, a well-designed cost function, and finally a physically meaningful initial point. As described in Ref. [12], a good candidate for the initial point is the free electron model-generated parameters for the coupling energies. We have also observed that using other zincblende structures' coupling parameters as initial points produced good results.

We have built our cost function to take into account both energy levels and effective masses at the same time. Since the cost comprises of points and curvatures to fit, this ensures a physically meaningful band diagram when initiated from the points described above. Following the definition of this cost function, we perform constrained nonlinear optimization using the Nelder–Mead simplex algorithm [14]. Other optimization methods such as genetic algorithms are found to be inefficient for this approach since the problem structure is sufficiently bounded and thus does not need a high level of exploration.

Results

Using the model described above, here we present the electronic band structure and the corresponding density of states calculated for 3C-SiC. Table 2 shows a comparison between the experimental values of high symmetry points
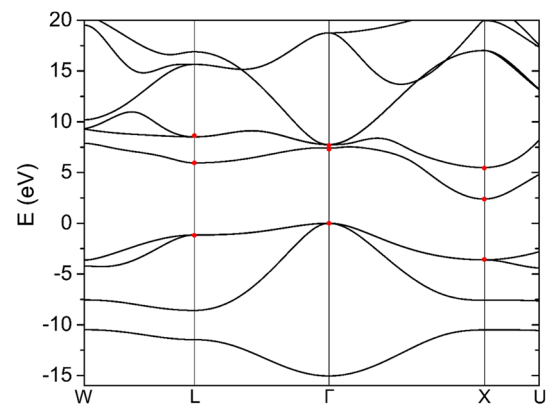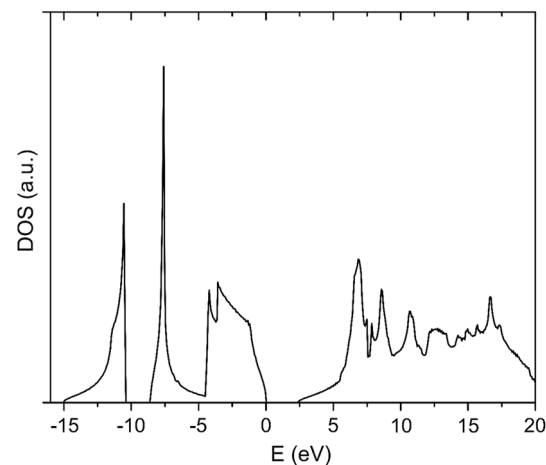

Fig. 3 Electronic band structure for SiC calculated with the $sp^3d^5s* + \Delta$ model. Experimental values reported in Ref. [6] are noted with red dots

Fig. 4 Density of states of SiC calculated with the $sp^3d^5s* + \Delta$ model described in this work

Table 3 Fitting parameters optimized for GaAs and SiC

Parameter	GaAs	SiC
a	5.6532 Å	4.3596 Å
E_{s_a}	−6.0533	−0.8766
E_{s_c}	−0.3340	−0.3421
E_{p_a}	3.3063	0.5489
E_{p_c}	6.2866	5.4488
E_{d_a}	13.3395	22.9218
E_{d_c}	13.3327	14.7797
$E_{s_a^*}$	19.3982	21.4411
$E_{s_c^*}$	19.3982	24.3075
$V_{ss\sigma}$	−1.7167	−1.9875
$V_{s^*s^*\sigma}$	−3.9205	−1.5826
$V_{s_a^*s_c\sigma}$	−2.1479	−6.9155
$V_{s_a s_c^*\sigma}$	−1.3658	−0.7085
$V_{s_a p_c\sigma}$	2.6999	5.6044
$V_{s_c p_a\sigma}$	2.9036	4.6564
$V_{s_c^* p_a\sigma}$	2.2556	6.5528
$V_{s_a^* p_c\sigma}$	2.5823	5.0141
$V_{s_a d_c\sigma}$	−2.7144	−6.5282
$V_{s_c d_a\sigma}$	2.4623	−4.3586
$V_{s_a^* d_c\sigma}$	−0.6651	−0.2985
$V_{s_c^* d_a\sigma}$	−0.5404	−0.3126
$V_{pp\sigma}$	4.3807	6.9700
$V_{pp\pi}$	−1.3874	−2.2015
$V_{p_a d_c\sigma}$	−1.3147	−3.9538
$V_{p_c d_a\sigma}$	−1.5263	−6.0081
$V_{p_a d_c\pi}$	2.1184	1.4686
$V_{p_c d_a\pi}$	2.4926	3.1505
$V_{dd\sigma}$	−0.7282	−1.1553
$V_{dd\pi}$	1.6289	4.4417
$V_{dd\delta}$	−1.8121	−4.9623
$\Delta_a/3$	0.1630	0.0071
$\Delta_c/3$	0.0823	0.0030

and effective masses and the same values calculated using our model and a previous SETBM implementation from Theodorou et al. [6]. Figure 3 shows that the conduction band minimum is at X point giving an indirect band structure with a bandgap of 2.39 eV. The optimized model predicts the experimental results with a reasonably high average accuracy of 99.91%. Other than the high symmetry points, it can also be noticed that the band diagram shows a constant gap in the Λ direction between valence and conduction bands as expected from reflectivity measurements [15]. Coupling parameters optimized for 3C-SiC are listed in Table 2, while the density of states diagram is shown in Fig. 4.

Specifically, for the band diagram of 3C-SiC, the spin–orbit coupling does not play a major role as the splitting of the valence bands is 10.3 meV. The effect becomes more important when other physical parameters, such as dielectric function [6], are of interest. Mainly, not to lose the generality of the model,

this effect is included in all of the calculations, obtaining small spin–orbit coupling parameters (δ_a, δ_c) as expected (Table 3).

Conclusion

We have reported the full implementation of a semiempirical tight-binding model for zincblende 3C-SiC with $sp^3 d^5 s*$ orbitals and spin–orbit coupling (Δ). Model parameters initialized using free electron model parameters and optimized using experimental energy values and effective masses have shown 99.91% average accuracy. Construction of the matrix and the optimization procedure can be further applied to other materials, in describing their electronic properties.

References

1. Harris, G.L.: Properties of Silicon Carbide. INSPEC, London (1995)
2. Shur, M., Rumyantsev, S., Levinshtein, M.: SiC Material and Devices. World Scientific, Singapore (2006)
3. Fan, J., Chu, P.K.-H.: Silicon Carbide Nanostructures. Springer, Berlin (2014)
4. Saddow, S.E., Agarwal, A.: Advances in Silicon Carbide Processes and Applications. Artech House, Norwood (2004)
5. Kackell, P., Wenzien, B., Bechstedt, F.: Phys. Rev. B **50**, 10761 (1994)
6. Theodorou, G., Tsegas, G., Kaxiras, E.: J. Appl. Phys. **85**, 2179 (1999)
7. Lubinsky, A.R., Ellis, D.E., Painter, G.S.: Phys. Rev. B **11**, 1534 (1974)
8. Junginger, H.-G., van Haeringen, G.: Physica Status Solidi **37**, 709 (1970)
9. Hemstreet, L.A., Fong, C.Y.: Phys. Rev. B **6**, 1464 (1972)
10. Vogl, P., Halmarson, H.P., Dow, J.D.: J. Phys. Chem. Solids **44**, 365 (1981)
11. Slater, J.C., Koster, G.F.: Phys. Rev. **94**, 1498 (1954)
12. Jancu, J.M., Sholz, R., Beltram, F., Bassani, F.: Phys. Rev. B **57**, 6493 (1998)
13. Datta, S.: Quantum Transport: Atom to Transistor. Cambridge University Press, Cambridge (2005)
14. Lagarias, J.C., Reeds, J.A., Wright, M., Wright, P.E.: Soc. Ind. Appl. Math. J. Optim, **9**, 112 (1998)
15. Madelung, O., von der Osten, W., Rossler, U.: Intrinsic Properties of Group IV Elements and III-V, II-VI and I-VII Compounds. Springer, Berlin (1987)